AIMS Mathematics, 9(9): 24271–24296.
DOI: 10.3934/math.20241181
Received: 17 June 2024
Revised: 05 August 2024
Accepted: 05 August 2024
Published: 16 August 2024

https://www.aimspress.com/journal/Math

Research article

Dynamics of a nonlinear state-dependent feedback control ecological model with fear effect

Zhanhao Zhang[1] **and Yuan Tian**[1,2,*]

[1] School of Mathematics and Statistics, Hubei Minzu University, Enshi, 445000, China
[2] Hubei Key Laboratory of Biologic Resources Protection and Utilization, Hubei Minzu University, Enshi, 445000, China

* **Correspondence:** Email: tyhbzjsx@163.com; Tel: +8618694036587.

Abstract: Integrated pest management is a pest control strategy that combines biological and chemical methods to reduce environmental pollution and protect biodiversity. Recent research indicated that the fear caused by predators had a significant effect on the growth, development, and reproductive processes of prey. Therefore, we have proposed a pest-natrual enemy system, which is a nonlinear state-dependent feedback control model that incorporated the fear effect in the predator-prey relationship. We discussed impulsive sets and phase sets of the model and derived an expression for the Poincaré map. Furthermore, we analyzed the existence and stability of order-1 periodic solutions and explored the existence of order-k ($k \geq 2$) periodic solutions. Finally, numerical simulations were conducted to validate our theoretical results and reveal their biological implications.

Keywords: integrated pest management; Poincaré map; periodic solution; existence and stability; fear effect
Mathematics Subject Classification: 34D23, 37N25, 93C27

1. Introduction

The relationship between predation and prey is one of the focal points in ecological research. As is well known, Lotka and Volterra independently proposed the famous Lotka-Volterra model, which has played an important role in describing the relationship between predators and prey [1]. However, as the model was applied in practice, scientists discovered that it also had some shortcomings, which are mainly reflected in the assumption that the number of prey eaten by a predator per unit time is linearly related, and this assumption is not reasonable when the number of prey is large. To address these issues, many scholars have improved the Lotka-Volterra model and introduced various functional response functions that more accurately simulate predation phenomena and made the model closer to

reality [2–5]. In addition to the relationships of predation and prey, intraspecific competition is also an important factor affecting the change of biological populations, so many researchers have taken into account intraspecific competition while analyzing the interactions between species [6–8].

Predators play a crucial role in ecosystems, shaping communities through a chain reaction of "who eats whom". However, recent research has revealed that the fear of being "eaten" can impact individual behaviors and even entire ecosystems, not just the act of being consumed. Zanette et al. conducted simulations on song sparrows and observed that predator-induced fear led to a significant reduction (up to 40%) in the number of offspring produced by these sparrows [9]. Similar evidence exists for other bird species [10–14], elk [15], snowshoe hare [16], and dugongs [17], demonstrating the impact of fear on population size. Insects can also be influenced by natural enemies. For instance, researchers demonstrated that the presence of a natural enemy causes two species of dragonflies, Enallagma cyathigerum and Ischnura rufostigma, to reduce their food intake, resulting in slower growth rates [18]. When aphids detect the presence of their natural enemy Hippodamiaconvergens, they produce more winged aphids as a defense mechanism against predation by Hippodamiaconvergens [19]. Furthermore, it was discovered that even after the departure of Hippodamiaconvergens, aphids continue to sense its scent and consequently increase the production of winged aphid offspring [20]. As a result, numerous scholars have conducted research on prey-predator relationships incorporating fear effects and have obtained rich biological conclusion [21–23].

In 2016, Wang, Zanette, and Zou proposed a predator–prey model incorporating the cost of fear into prey reproduction [24], and the model is as follows:

$$\begin{cases} \dfrac{dx}{dt} = \dfrac{r_0 x}{1+ky} - dx - ax^2 - \dfrac{pxy}{1+qx}, \\ \dfrac{dy}{dt} = \dfrac{cpxy}{1+qx} - my. \end{cases} \tag{1.1}$$

where $x(t)$ and $y(t)$ denote the population densities of prey and predators, and r_0 is the intrinsic growth rate of the prey. In addition, d is the natural mortality rate of the prey and a denotes the mortality rate due to intraspecific competition of the prey, and k denotes the level of fear (the level of fear reflected in the prey's fear of the predator and, hence, anti-predator behavior). $\frac{px}{1+qx}$ is the Holling type II functional response function, c is the efficiency of biological energy conversion, and m represents the mortality rate of predators. The dynamical behaviour of the system (1.1) has been studied detailedly in literature [24].

Integrated pest management (IPM) was first proposed by the Food and Agriculture Organization of the United Nations in 1996. IPM is a comprehensive approach to pest management that utilizes appropriate techniques and methods based on the population dynamics of pests and their environmental relationships, aiming to maintain pest populations below the economic threshold. IPM includes chemical control (spraying pesticide), biological control (the utilization of biometabolites, parasites), agricultural control (crop rotation, adjustment of planting periods), physical control measures, and more. In recent years, agricultural monitoring and early warning, model prediction, optimal control, and complex network technologies have played an important role in protecting the ecological environment and promoting agricultural development [25–29]. IPM uses information technology to achieve more intelligent agricultural production management. Some scholars have developed biological mathematical models based on the biological background and mathematical principles of

IPM [30–33]. In these IPM models, differential systems with state-dependent impulses exhibits both continuous and discrete characteristics. Therefore, it is very suitable for portraying the interaction between pests and natural enemies, pesticide spraying, releasing of natural enemies, and so on. Literature [34–36] shows that the state-dependent feedback control model can effectively analyze the dynamic behavior of pests and natural enemies under the interference of the external environment and provide a theoretical basis for establishing a more optimized control strategy.

In the context of the above knowledge, we take the integrated control tactics into account for model (1.1). Then, model (1.1) becomes:

$$\begin{cases} \left.\begin{aligned} \frac{dx(t)}{dt} &= \frac{r_0 x}{1+ky} - dx - ax^2 - \frac{pxy}{1+qx}, \\ \frac{dy(t)}{dt} &= \frac{cpxy}{1+qx} - my, \end{aligned}\right\} & x(t) < E_T, \\ \left.\begin{aligned} x(t^+) &= \left[1 - \frac{\delta x(t)}{x(t)+\beta}\right] x(t), \\ y(t^+) &= y(t) + \frac{\tau}{1+\theta y(t)}, \end{aligned}\right\} & x(t) = E_T. \end{cases} \tag{1.2}$$

If the density of the pest population is below the economic threshold E_T, the pest-predator system is not affected by external chemical and biological control, and the first two equations of (1.2) reflect the rate of change of the pest and predator in their interactions within this stage. Once the density of the pest population reaches E_T, we take chemical and biological approaches, i.e., spraying insecticides and releasing natural enemies at the same time. The third equation of system (1.2) indicates that the density of pests is impulsive reduced to $(1 - \frac{\delta x(t)}{x(t)+\beta})x(t)$ by poisoning with chemicals, and the fourth equation of system (1.2) means that the density of natural enemies is impulsive increased to $y(t) + \frac{\tau}{1+\theta y(t)}$ by artificial breeding and releases. Here, $\delta > 0$ is defined as the maximum kill rate of the pests with the use of insecticides, $\beta > 0$ is the half-saturation constant, and $\theta > 0$ denotes the parameter for regulating the density of the natural enemy. $\tau > 0$ is the number of natural enemies to be released. Obviously, τ is the maximum number of natural enemies released. The third and fourth equations of system (1.2) reflect the density dependence of the implementation of the control strategy. Some previous models mainly focus on the linear impulses, in which the number of natural enemies released is a constant in the models no matter how large the natural enemies and pests remain in the field. However, in this work, we introduced the nonlinear state-dependent feedback control strategy, which shows that the instant killing rate of insecticide and the number of natural enemies released depend on their density, and this is the characteristic of system (1.2). Combined with the "fear effect" of biological populations, next we will study the global dynamical behavior of the model (1.2) and to reveal how the main parameters of the model (1.2) affect the dynamics of the system.

To do this, we first summarize the key properties of the corresponding ordinary differential equation (ODE) system (1.1) in the case of no external interference, and then construct the impulsive sets and phase sets in relation to impulsive differential equations (1.2) by using the basic theory of the impulsive semi-dynamic system. The existence and stability of order-1 periodic solutions for $\tau = 0$ and $\tau > 0$ have been addressed and the existence of order-k ($k > 1$) periodic solutions are discussed. Furthermore, numerical simulations are conducted to validate our theoretical findings, and biological significance are discussed. All the results can help us to further understand and give insight into the dynamic complexity

of the predator-prey biological system with nonlinear impulsive control.

2. Analytical formula and properties for the Poincaré map

The main conclusions of literature [24] for the equilibrium point of system (1.1) are summarized as follows:

Lemma 2.1. *(i) The trivial equilibrium $E_0 = (0,0)$ is unstable and the boundary equilibrium $E_1 = (\frac{r_0-d}{a}, 0)$ is locally asymptotically stable if $r_0 > d$ and $(r_0 - d)(cp - mq) < am$;*
(ii) The trivial equilibrium $E_0 = (0,0)$ is unstable and the boundary equilibrium E_1 is globally asymptotically stable if the inequality $r_0 > d$ and $cp \le mq$ are satisfied.

If $(cpr_0 - cpd - am)(cp - mq) > aqm^2$, then the positive equilibrium point $E_2 = (x_2, y_2)$ exists for system (1.1), in which

$$x_2 = \frac{m}{cp - mq}, \quad y_2 = \frac{-(p + dk + dkqx_2 + akx_2 + akqx_2^2) + \sqrt{\Delta_2}}{2pk},$$

where

$$\Delta_2 = (p + dk + dkqx_2 + akx_2 + akqx_2^2)^2 + 4pk(r_0 + r_o qx_2 - d - dqx_2 - ak - aqx_2^2).$$

Lemma 2.2. *The positive equilibrium E_2 is locally asymptotically stable if*

$$\frac{am}{cp - mq} < r_0 - d \le \frac{a(cp + mq)}{q(cp - mq)} \tag{2.1}$$

or

$$\begin{cases} r_0 - d > \dfrac{a(cp + mq)}{q(cp - mq)}, \\ k > \dfrac{q(cp - mq)^2[(r_0 - d)q(cp - mq) - a(cp + mq)]}{c^2 pa[qd(cp - mq) + a(cp + mq)]}. \end{cases} \tag{2.2}$$

is satisfied.

Lemma 2.3. *The positive equilibrium E_2 is globally asymptotically stable if*

$$\frac{am}{cp - mq} < r_0 - d \le \frac{a(cp + mq)}{q(cp - mq)} \quad \text{and} \quad \frac{r_0 q}{cp - mq} \ge 1. \tag{2.3}$$

We summarize the equilibrium points of system (1.1) and their stability in Table 1.

Table 1. Stability of the equilibrium points.

Points	$r_0 > d$, $cp \le mq$	$cp > mq$, $0 < r_0 - d < \frac{am}{cp-mq}$	$cp > mq$, $\frac{am}{cp-mq} < r_0 - d \le \frac{a(cp+mq)}{q(cp-mq)}$
$E_0 = (0,0)$	unstable	unstable	unstable
$E_1 = (\frac{r_0-d}{a}, 0)$	stable	stable	unstable
$E_2 = (x_2, y_2)$	does not exist	does not exist	stable

2.1. Impulsive set

In order to derive the analytical form of the Poincaré map and investigate the dynamics of model (1.2), we first focus on the precise domains of the impulsive set and phase set of model (1.2).

As shown in Figure 1, we define two straight lines related to economic thresholds: $L_1 : x = E_T$, $L_2 : x = (1 - H)E_T$, where $H = \frac{\delta E_T}{E_T+\beta}$. The two isoclines of system (1.2) are denoted by L_3 and L_4, in which

$$L_3 : y = \frac{-(p + dk + dkqx + akx + akqx^2) + \sqrt{\Delta}}{2pk} \quad L_4 : x = \frac{m}{cp - mq}$$

where

$$\Delta = (p + dk + dkqx + akx + akqx^2)^2 + 4pk(r_0 + r_o qx - d - dqx - ak - aqx^2)$$

Next, we will discuss the impulsive set and phase set of system (1.2) if the positive equilibrium point $E_2 = (x_2, y_2)$ is globally asymptotically stable for system (1.1).

Denote the point $E_3 = (x_{E_3}, y_{E_3})$ as the intersection point of the trajectory τ_1 with the line L_3. If line L_2 intersects τ_1, the intersections of τ_1 with L_2 are $B_1 = (x_{B_1}, y_{B_1})$ and $B_2 = (x_{B_2}, y_{B_2})$, and τ_1 is tangent to the line L_1 at point $T = (x_T, y_T)$. If the trajectory τ_2 is tangent to the line L_2, then denote the tangent point as $C_0 = (x_{C_0}, y_{C_0})$ and point $C_1 = (x_{C_1}, y_{C_1})$ as the intersection of the trajectory τ_2 with the line L_1, as shown in Figure 1(A).

It is easy to see that in Figure 1(A), if $E_T > x_2$, the line L_1 is to the right of the point E_2. In Figure 1(B), if $E_T < x_2$, the line L_1 is to the left of the point E_2. In order to facilitate the discussion of the impulsive set and phase set of system (1.2) in different cases, we divide the relationship between E_T and x_2 into the following two cases:

$$A_1 : E_T > x_2, \qquad A_2 : E_T \leq x_2,$$

and consider the relationship between $(1 - H)E_T$ and x_{E_3} into the following two cases:

$$(1) : (1 - H)E_T \geq x_{E_3}, \qquad (2) : (1 - H)E_T < x_{E_3}.$$

For system (1.2), define two impulsive sets as follows:

$$\mathcal{I} = \{(x, y) \in R_+^2 \mid x = E_T, 0 \leq y \leq y_T\}. \tag{2.4}$$

and

$$\mathcal{I}_0 = \{(x, y) \in R_+^2 \mid x = E_T, 0 \leq y \leq y_{c_1}\}. \tag{2.5}$$

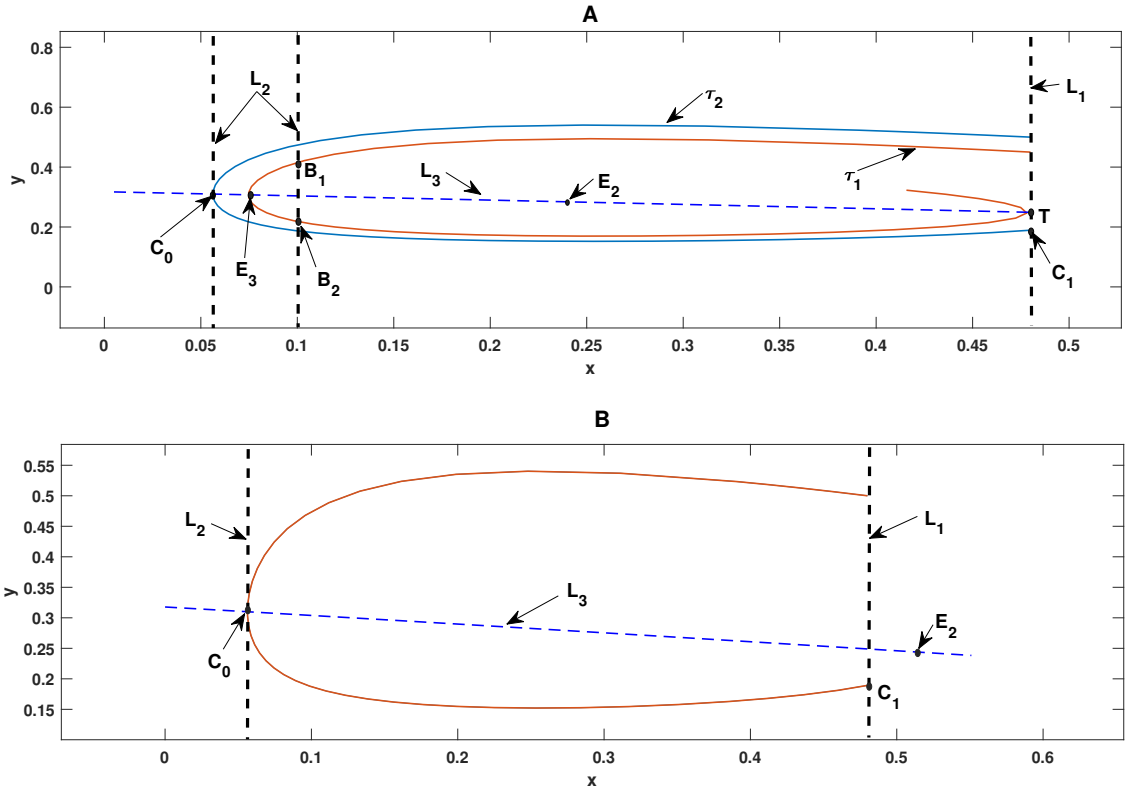

Figure 1. The definitions of impulsive sets and phase sets are related to the positional relationship between two straight lines L_1 and L_2 for case A_1 and case A_2.

As shown in Figure 1(A), if $(1-H)E_T > x_{E_3}$, τ_1 is tangent to L_1 at point T, arbitrary trajectory starting from point $G = ((1-H)E_T, y_G)$, $y_G \in (y_{B_2}, y_{B_1})$ will not eventually reach the line L_1, then we have the following results:

Lemma 2.4. *For case $A_1(1)$, any solution starting from the point $(x_0^+, y_0^+) \in L_2$ with $y_0^+ \in (y_{B_2}, y_{B_1})$ does not experience pulse effects.*

Based on the above definition, we define the impulsive sets in different cases.

Lemma 2.5. *For case $A_1(1)$, the impulsive set is $\mathcal{I}$, and the impulsive set is $\mathcal{I}_0$ for case $A_1(2)$. For case A_2, the impulsive set is $\mathcal{I}_0$.*

Proof. According to Lemma 2.4, for case $A_1(1)$, any solution of system (1.2) initiating from the set $\{(x, y) \mid x = (1-H)E_T, y \in (y_{B_2}, y_{B_1})\}$ will not reach the line L_1 and will be free from the pulse effect, which also implies that the impulsive set is $\mathcal{I}$. For case $A_1(2)$, it is easy to see that any solution of system (1.2) starting from the line L_2 can only be below point T upon reaching line L_1, which indicates that the impulsive set is $\mathcal{I}_0$. Applying the same method of analysis to case A_2 also yields that the impulsive set is $\mathcal{I}_0$ (as shown in Figure 1(B)). This completes the proof.

□

2.2. Phase set

According to the proof of Lemma 2.4, define the following set for case $A_1(1)$:

$$D_0 = [0, y_{B_2}] \cup [y_{B_1}, +\infty). \tag{2.6}$$

Moreover, the study of the properties of impulsive function $y(t^+) = y(t) + \dfrac{\tau}{1+\theta y(t)}$ is the key to determinating the phase set, so the impulsive function can be described as

$$f(z) = z + \frac{\tau}{1+\theta z}, \quad z \in [0, y_T]. \tag{2.7}$$

Taking the derivative of function $f(z)$: $f'(z) = 1 - \dfrac{\tau\theta}{(1+\theta z)^2}$ and $f'(z) = 0$ at $z = \dfrac{\sqrt{\tau\theta}-1}{\theta}$. By the way, we denote the useful point: $V = (x_V, y_V) = (E_T, \frac{\sqrt{\tau\theta}-1}{\theta})$, and the point V is located in the impulsive set. It will map to impulsive point $V^+ = (x_{V^+}, y_{V^+}) = ((1-H)E_T, \frac{2\sqrt{\tau\theta}-1}{\theta})$ after one impulsive effect.

Then, we will discuss the monotonicity of the function $f(z)$ and consider the exact phase set of the different cases.

For case $A_1(1)$, we have known that the impulsive set in this case is $\mathcal{I} = \{(x, y) \in R_+^2 \mid x = E_T, 0 \le y \le y_T\}$, then according to the monotonicity of $f(z)$, the phase set will be discussed under different conditions:

(I) $\frac{\sqrt{\tau\theta}-1}{\theta} \le 0$. We can get that $f'(z) \ge 0$ for all $z \in [0, y_T]$, which implies that the function $f(z)$ is monotonically increasing. We denote

$$D_1^0 = [\tau, y_T + \frac{\tau}{1+\theta y_T}], \quad D_1 = D_0 \cap D_1^0.$$

Then, the phase set under the condition $A_1(1)$ (I) is

$$\mathcal{X}_1 = \{(x^+, y^+) \in R_+^2 \mid x^+ = (1-H)E_T, y^+ \in D_1\}$$

(II) $\frac{\sqrt{\tau\theta}-1}{\theta} \ge y_T$. Derivative function $f'(z) \le 0$ for $z \in [0, y_T]$, thus $f(z)$ is monotonically decreasing and $y_T + \frac{\tau}{1+\theta y_T} \le f(z) \le \tau$. We denote

$$D_2^0 = [y_T + \frac{\tau}{1+\theta y_T}, \tau], \quad D_2 = D_0 \cap D_2^0.$$

Then, the phase set under the condition $A_1(1)$ (II) is

$$\mathcal{X}_2 = \{(x^+, y^+) \in R_+^2 \mid x^+ = (1-H)E_T, y^+ \in D_2\}$$

(III) $0 < \frac{\sqrt{\tau\theta}-1}{\theta} \le y_T$. If $0 < z \le \frac{\sqrt{\tau\theta}-1}{\theta}$, then $f'(z) \le 0$ and the function $f(z)$ is monotonically decreasing. Thus, $\frac{2\sqrt{\tau\theta}-1}{\theta} \le f(z) < \tau$ and we denote

$$D_3^0 = [\frac{2\sqrt{\tau\theta}-1}{\theta}, \tau), \quad D_3 = D_0 \cap D_3^0.$$

If $\frac{\sqrt{\tau\theta}-1}{\theta} < z \leq y_T$, $f^{'}(z) > 0$, and the function $f(z)$ is monotonically increasing. Thus, $\frac{2\sqrt{\tau\theta}-1}{\theta} < f(z) \leq y_T + \frac{\tau}{1+\theta y_T}$ and we denote

$$D_4^0 = (\frac{2\sqrt{\tau\theta}-1}{\theta}, y_T + \frac{\tau}{1+\theta y_T}], \quad D_4 = D_0 \cap D_4^0.$$

Now, under the conditions of case $A_1(1)$ (III), the impulsive set is $\mathcal{I} = \mathcal{I}_1 \cup \mathcal{I}_2$, where

$$\mathcal{I}_1 = \{(x,y) \in R_+^2 \mid x = E_T, 0 < y \leq \frac{\sqrt{\tau\theta}-1}{\theta}\}$$

and

$$\mathcal{I}_2 = \{(x,y) \in R_+^2 \mid x = E_T, \frac{\sqrt{\tau\theta}-1}{\theta} < y \leq y_T\}.$$

The corresponding phase set of impulsive set $\mathcal{I} = \mathcal{I}_1 \cup \mathcal{I}_2$ is $\mathcal{X}_3 \cup \mathcal{X}_4$, where

$$\mathcal{X}_3 = \{(x^+,y^+) \in R_+^2 \mid x^+ = (1-H)E_T, y^+ \in D_3\}$$

and

$$\mathcal{X}_4 = \{(x^+,y^+) \in R_+^2 \mid x^+ = (1-H)E_T, y^+ \in D_4\}.$$

For case $A_1(2)$, it can be seen that the impulsive set is $\mathcal{I}_0$, then based on the monotonicity of the function $f(z)$, the phase set will be discussed as follows:

(I) $\frac{\sqrt{\tau\theta}-1}{\theta} \leq 0$. We know that $f^{'}(z) \geq 0$ for all $z \in [0, y_{C_1}]$, which implies that the function $f(z)$ is monotonically increasing, i.e., $\tau \leq f(z) \leq y_{C_1} + \frac{\tau}{1+\theta y_{C_1}}$, so the phase set can be defined as:

$$\mathcal{X}_5 = \{(x^+,y^+) \in R_+^2 \mid x^+ = (1-H)E_T, y^+ \in D_5\}$$

where

$$D_5 = [\tau, y_{C_1} + \frac{\tau}{1+\theta y_{C_1}}].$$

(II) $\frac{\sqrt{\tau\theta}-1}{\theta} \geq y_{C_1}$. We know that $f^{'}(z) \leq 0$ for $z \in [0, y_{C_1}]$, thus the function $f(z)$ is monotonically decreasing and $y_{C_1} + \frac{\tau}{1+\theta y_{C_1}} \leq f(z) \leq \tau$. The phase set is defined as

$$\mathcal{X}_6 = \{(x^+,y^+) \in R_+^2 \mid x^+ = (1-H)E_T, y^+ \in D_6\}$$

where

$$D_6 = [y_{C_1} + \frac{\tau}{1+\theta y_{C_1}}, \tau].$$

(III) $0 < \frac{\sqrt{\tau\theta}-1}{\theta} \leq y_{C_1}$. If $0 < z \leq \frac{\sqrt{\tau\theta}-1}{\theta}$, then $f^{'}(z) \leq 0$ and the function $f(z)$ is monotonically decreasing. We denote:

$$D_7 = [\frac{2\sqrt{\tau\theta}-1}{\theta}, \tau).$$

If $\frac{\sqrt{\tau\theta}-1}{\theta} < z \leq y_{C_1}$, then $f^{'}(z) > 0$ and the function $f(z)$ is monotonically increasing, then

$$D_8 = (\frac{2\sqrt{\tau\theta}-1}{\theta}, y_{C_1} + \frac{\tau}{1+\theta y_{C_1}}].$$

Under the condition $A_1(2)$ (III), the impulsive set is $\mathcal{I}_0 = \mathcal{I}_1 \cup \mathcal{I}_3$, where

$$\mathcal{I}_3 = \{(x, y) \in R_+^2 \mid x = E_T, \frac{\sqrt{\tau\theta} - 1}{\theta} < y \leq y_{C_1}\}.$$

The corresponding phase set of impulsive set $\mathcal{I}_0 = \mathcal{I}_1 \cup \mathcal{I}_3$ is $\mathcal{X}_7 \cup \mathcal{X}_8$, where

$$\mathcal{X}_7 = \{(x^+, y^+) \in R_+^2 \mid x^+ = (1 - H)E_T, y^+ \in D_7\}$$

and

$$\mathcal{X}_8 = \{(x^+, y^+) \in R_+^2 \mid x^+ = (1 - H)E_T, y^+ \in D_8\}.$$

For case A_2, the phase sets can be analyzed in a similar way as described in case $A_1(2)$, then we have:

(I) $\frac{\sqrt{\tau\theta}-1}{\theta} \leq 0$. The phase set is $\mathcal{X}_5$.

(II) $\frac{\sqrt{\tau\theta}-1}{\theta} \geq y_{C_1}$. The phase set is $\mathcal{X}_6$.

(III) $0 < \frac{\sqrt{\tau\theta}-1}{\theta} \leq y_{C_1}$. The phase set is $\mathcal{X}_7 \cup \mathcal{X}_8$.

For the sake of convenience, and to explore the complexity of the system (1.2) under varying parameters more clearly such as E_T, τ, δ, etc., we summarized the impulsive sets and phase sets for different cases as follows in Table 2:

Table 2. Impulsive sets and phase sets in different cases.

Cases		Impulsive set	Phase set
$A_1(1)$	(I)	$\mathcal{I}$	$\mathcal{X}_1$
	(II)	$\mathcal{I}$	$\mathcal{X}_2$
	(III)	$\mathcal{I} = \mathcal{I}_1 \cup \mathcal{I}_2$	$\mathcal{X}_3 \cup \mathcal{X}_4$
$A_1(2)$	(I)	$\mathcal{I}_0$	$\mathcal{X}_5$
	(II)	$\mathcal{I}_0$	$\mathcal{X}_6$
	(III)	$\mathcal{I}_0 = \mathcal{I}_1 \cup \mathcal{I}_3$	$\mathcal{X}_7 \cup \mathcal{X}_8$
A_2	(I)	$\mathcal{I}_0$	$\mathcal{X}_5$
	(II)	$\mathcal{I}_0$	$\mathcal{X}_6$
	(III)	$\mathcal{I}_0 = \mathcal{I}_1 \cup \mathcal{I}_3$	$\mathcal{X}_7 \cup \mathcal{X}_8$

2.3. Poincaré map

Consider the Poincaré map in case $A_1(2)$. First, the defining two sections are as follows:

$$S_{E_T} = \{(x, y) \mid x = E_T, y \geq 0\}, \quad S_{\delta E_T} = \{(x, y) \mid x = (1 - H)E_T, y \geq 0\}.$$

Point $Q_k^+ = ((1 - H)E_T, y_{Q_k^+})$ is located on the line L_2, and the trajectory of system (1.2) passing through Q_k^+ will reach S_{E_T}, i.e., the trajectory initiating from Q_k^+ will arrive at line L_1, and the intersection of the trajectory with line L_1 is $Q_{k+1} = (E_T, y_{Q_{k+1}}) \in S_{E_T}$. After one time impulsive effect, Q_{k+1} will map to $Q_{k+1}^+ = ((1 - H)E_T, y_{Q_{k+1}}^+)$ with $y_{Q_{k+1}}^+ = y_{Q_{k+1}} + \frac{\tau}{1+\theta y_{Q_{k+1}}}$ on $S_{\delta E_T}$. Thus, we can define $P(y_{Q_k}^+) = y_{Q_{k+1}}$ and the Poincaré map P_M as

$$y_{Q_{k+1}}^+ = y_{Q_{k+1}} + \frac{\tau}{1 + \theta y_{Q_{k+1}}} = P(y_{Q_k}^+) + \frac{\tau}{1 + \theta P(y_{Q_k}^+)} = P_M(y_{Q_k}^+). \tag{2.8}$$

Further, noting that

$$P(x,y)=\frac{r_0x}{1+ky}-dx-ax^2-\frac{pxy}{1+qx},\quad Q(x,y)=\frac{cpxy}{1+qx}-my,$$

then

$$\begin{cases}\dfrac{dy}{dx}=\dfrac{Q(x,y)}{P(x,y)}=\dfrac{\dfrac{cpxy}{1+qx}-my}{\dfrac{r_0x}{1+ky}-dx-ax^2-\dfrac{pxy}{1+qx}}=g(x,y),\\ y((1-H)E_T)=y_0^+,\end{cases}\tag{2.9}$$

For model (2.9), we only focus on the region

$$\Omega=\{(x,y)\mid x>0,y>0,y<\frac{-(p+dk+dkqx+akx+akqx^2)+\sqrt{\Delta}}{2pk}\}.\tag{2.10}$$

where

$$\Delta=(p+dk+dkqx+akx+akqx^2)^2+4pk(r_0+r_oqx-d-dqx-ak-aqx^2).$$

Noting the point $C_0=((1-H)E_T,y_{C_0})\in S_{\delta E_T}$ with

$$y_{C_0}=\frac{-(p+dk+dkq(1-H)E_T+ak(1-H)E_T+akq(1-H)^2E_T^2)+\sqrt{\Delta_1}}{2pk}$$

where

$$\Delta_1=(p+dk+dkqx_t+akx_t+akqx_t^2)^2+4pk(r_0+r_oqx_t-d-dqx_t-ak-aqx_t^2),\quad x_t=(1-H)E_T.$$

The initial value of model (2.9) is $x_0^+=(1-H)E_T$, $y_0^+=S$ with $S<y_{C_0}$(i.e., $(x_0^+,y_0^+)\in\Omega$), then we have

$$y(x,S)=S+\int_{(1-H)E_T}^{x}g(s,y(s,S))ds.\tag{2.11}$$

Thus, the Poincaré map P_M in the region Ω is

$$P_M(S)=y(E_T,S)+\frac{\tau}{1+\theta y(E_T,S)}.\tag{2.12}$$

3. Existence and stability of the boundary order-1 periodic solution for $\tau=0$

If $\tau=0$, then we consider the following subsystem:

$$\begin{cases}\dfrac{dx}{dt}=r_0x-dx-ax^2,x<E_T,\\ x(t^+)=\left(1-\dfrac{\delta x(t)}{x(t)+\beta}\right)x(t),x=E_T.\end{cases}\tag{3.1}$$

The initial condition for system (3.1) is $x(0^+)=(1-H)E_T$, and solving the first equation of the system (3.1):

$$x^T(t)=\frac{Fe^{(r_0-d)t}(r_0-d)}{a(1+Fe^{(r_0-d)t})}\tag{3.2}$$

where

$$F = \frac{a(1-H)E_T}{r_0 - d - a(1-H)E_T}$$

If the trajectory $x^T(t)$ reaches L_1, letting $E_T = \frac{Fe^{(r_0-d)T}(r_0-d)}{a(1+Fe^{(r_0-d)T})}$, we have

$$T = \frac{\ln(\frac{aE_T}{F(r_0-d-aE_T)})}{r_0 - d}.$$

Therefore, there exists a boundary order-1 periodic solution $(x^T(t), 0) = (\frac{Fe^{(r_0-d)t}(r_0-d)}{a(1+Fe^{(r_0-d)t})}, 0)$ for system (1.2), and we have the following conclusions about the stability of $(x^T(t), 0)$.

Theorem 3.1. *The boundary order-1 periodic solution $(x^T(t), 0)$ is orbitally asymptotically stable if, and only if,*

$$0 < \delta < \frac{(E_T+\beta)(r_0-d-aE_T)}{aE_T^2 exp(A')} - \frac{(E_T+\beta)(r_0-d)}{aE_T^2} + 1 + \frac{\beta}{E_T}, \tag{3.3}$$

where

$$A' = (r_0 - d - m)T + 2\ln(\frac{1+F}{1+F(e^{(r_0-d)T})}) + \frac{cp}{q(r_0-d)+a}\ln(\frac{[q(r_0-d)+a]Fe^{(r_0-d)T}+a}{[q(r_0-d)+a]F+a}).$$

Proof. Denoting

$$P(x,y) = \frac{r_0 x}{1+ky} - dx - ax^2 - \frac{pxy}{1+qx}, \quad Q(x,y) = \frac{cpxy}{1+qx} - my,$$

$$\alpha(x,y) = -\frac{\delta x^2(t)}{x(t)+\beta}, \quad \varphi(x,y) = \frac{\tau}{1+\theta y(t)}, \quad \phi(x,y) = x - E_T.$$

By calculating:

$$\frac{\partial P}{\partial x} = \frac{r_0}{1+ky} - d - 2ax - \frac{py(1+qx) - pqxy}{(1+qx)^2}, \quad \frac{\partial Q}{\partial y} = \frac{cpx}{1+qx} - m,$$

$$\frac{\partial \alpha}{\partial x} = -\frac{\delta x^2 + 2\delta\beta x}{(x+\beta)^2}, \quad \frac{\partial \varphi}{\partial y} = -\frac{\tau\theta}{(1+\theta y)^2}, \quad \frac{\partial \phi}{\partial x} = 1,$$

$$\frac{\partial \alpha}{\partial y} = \frac{\partial \varphi}{\partial x} = \frac{\partial \phi}{\partial y} = 0, \quad (x^T(T), y^T(T)) = (E_T, 0), \quad (x^T(T^+), y^T(T^+)) = ((1-H)E_T, 0).$$

then

$$\begin{aligned}
\Delta_1 &= \frac{P_+(\frac{\partial \varphi}{\partial y}\frac{\partial \phi}{\partial x} - \frac{\partial \varphi}{\partial x}\frac{\partial \phi}{\partial y} + \frac{\partial \phi}{\partial x}) + Q_+(\frac{\partial \alpha}{\partial x}\frac{\partial \phi}{\partial y} - \frac{\partial \alpha}{\partial y}\frac{\partial \phi}{\partial x} + \frac{\partial \phi}{\partial y})}{P\frac{\partial \phi}{\partial x} + Q\frac{\partial \phi}{\partial y}} \\
&= \frac{(1-H)(1-\tau\theta)[r_0 - d - a(1-H)E_T]}{r_0 - d - aE_T} \\
&= \frac{(1-H)[r_0 - d - a(1-H)E_T]}{r_0 - d - aE_T} \\
&< \frac{r_0 - d - a(1-H)E_T}{r_0 - d - aE_T}
\end{aligned}$$

From the previous analysis on the existence of boundary order-1 periodic solution, we know that: $\Delta_1 > 0$.

$$
\begin{aligned}
&exp(\int_0^T [\frac{\partial P}{\partial x}(x^T(t), y^T(t)) + \frac{\partial Q}{\partial y}(x^T(t), y^T(t))]dt) \\
=&exp(\int_0^T [r_0 - d - 2a(\frac{Fe^{(r_0-d)t}(r_0-d)}{a(1+Fe^{(r_0-d)t})}) + \frac{cp(\frac{Fe^{(r_0-d)t}(r_0-d)}{a(1+Fe^{(r_0-d)t})}}{1+q(\frac{Fe^{(r_0-d)t}(r_0-d)}{a(1+Fe^{(r_0-d)t})}} - m]dt) \\
=&exp(\int_0^T [I_1 + I_2 + I_3]dt)
\end{aligned}
$$

where

$$
\begin{aligned}
I_1 = r_0 - d - m, \quad I_2 = -\frac{2(r_0-d)Fe^{(r_0-d)t}}{1+Fe^{(r_0-d)t}}, \\
I_3 = \frac{[cp(r_0-d)Fe^{(r_0-d)t}][a(1+Fe^{(r_0-d)t})]}{[a(1+Fe^{(r_0-d)t})][q(r_0-d)Fe^{(r_0-d)t} + a(1+Fe^{(r_0-d)t})]} \\
= \frac{cp(r_0-d)Fe^{(r_0-d)t}}{Fe^{(r_0-d)t}[q(r_0-d)+a]+a}.
\end{aligned}
$$

$$
\begin{aligned}
&exp(\int_0^T I_1 dt) = exp((r_0 - d - m)T), \\
&exp(\int_0^T I_2 dt) = exp(-2\ln(1+Fe^{(r_0-d)t})\Big|_0^T) = exp(2\ln(\frac{1+F}{1+F(e^{(r_0-d)T})})), \\
&exp(\int_0^T I_3 dt) = exp(\int_0^T \frac{cp(r_0-d)Fe^{(r_0-d)t}}{Fe^{(r_0-d)t}[q(r_0-d)+a]+a}dt) \\
&\qquad = exp(\frac{cp}{q(r_0-d)+a}\ln(Fe^{(r_0-d)t}[q(r_0-d)+a]+a)\Big|_0^T) \\
&\qquad = exp(\frac{cp}{q(r_0-d)+a}\ln(\frac{[q(r_0-d)+a]Fe^{(r_0-d)T}+a}{[q(r_0-d)+a]F+a})).
\end{aligned}
$$

Therefore, we have:

$$
exp(\int_0^T [I_1 + I_2 + I_3]dt) = exp(A')
$$

where

$$
A' = (r_0 - d - m)T + 2\ln(\frac{1+F}{1+F(e^{(r_0-d)T})}) + \frac{cp}{q(r_0-d)+a}\ln(\frac{[q(r_0-d)+a]Fe^{(r_0-d)T}+a}{[q(r_0-d)+a]F+a}).
$$

Then, the Floquet multiplier μ_2 can be obtained:

$$
\begin{aligned}
\mu_2 &= \Delta_1 exp(\int_0^T [\frac{\partial P}{\partial x}(x^T(t), y^T(t)) + \frac{\partial Q}{\partial y}(x^T(t), y^T(t))]dt) \\
&= \frac{(1-H)[r_0 - d - a(1-H)E_T]}{r_0 - d - aE_T} exp(A') \\
&< \frac{r_0 - d - a(1-H)E_T}{r_0 - d - aE_T} exp(A')
\end{aligned}
$$

Thus, it follows from (3.3) that $|\mu_2| < 1$, and the boundary order-1 periodic solution $(x^T(t), 0)$ is orbitally asymptotically stable. This completes the proof. □

4. Existence and stability of the order-1 periodic solution for $\tau > 0$

Previously, the impulsive sets and phase sets under different conditions are plotted in Table 2 and the boundary order-1 periodic solution for $\tau = 0$ has been discussed. Then, if $\tau > 0$, we will consider the existence and stability of the periodic solution for system (1.2).

Theorem 4.1. *For case $A_1(1)$(I) (or case $A_1(1)$(II)), if $y_{T^+} \geq y_{B_1}$, there exists at least one fixed point of the Poincaré map $P_M(y_i^+)$, i.e., there exists at least one order-1 periodic solution for the system (1.2); if $y_{T^+} < y_{B_1}$, $P_M(y_i^+)$ does not have any fixed point.*

Proof. For case $A_1(1)$, as shown in Figure 1, there exists a curve τ_1 intersecting the line L_2 at two points B_1 and B_2 and τ_1 is tangent to the line L_1 at point T. If $y_{T^+} = y_{B_1}$, then the curve $\widehat{B_1T}$ constitutes the order-1 periodic solution for system (1.2).

For case $A_1(1)$(I), if $y_{T^+} > y_{B_1}$, i.e., the point T^+ is above the point B_1, we know that

$$P_M(y_{B_1}) > y_{B_1}. \tag{4.1}$$

Moreover, the trajectory from T^+ intersects the line L_1 at T_1 which lies below the point T, i.e., $y_{T_1} < y_T$. For case $A_1(1)$(I), the impulsive function $f(z)$ is monotonically increasing on the interval $[0, y_T]$, then $f(y_{T_1}) < f(y_T)$, i.e., $y_{T_1^+} < y_{T^+}$. The above results show that for case $A_1(1)$(I), the Poincaré map satisfies

$$P_M(y_{T^+}) < y_{T^+}. \tag{4.2}$$

It follows from (4.1) and (4.2) that there exists a fixed point of the Poincaré map on interval (y_{B_1}, y_{T^+}), i.e., there exists an order-1 periodic solution for system (1.2).

For case $A_1(1)$(I), if $y_{T^+} < y_{B_1}$, the impulsive point will be located on the phase set with $y_i^+ \in [\tau, y_{T^+}]$. According to Lemma 2.4, we know that any solution of system (1.2) will undergo a finite number of impulses and will not eventually reach the line L_1. Thus, there is no fixed point for system (1.2).

For case $A_1(1)$(II), if $y_{T^+} > y_{B_1}$, the inequality (4.1) holds. The highest impulsive point is denoted as $B_\tau = ((1 - H)E_T, \tau)$ that satisfies the inequality

$$P_M(\tau) < \tau. \tag{4.3}$$

It follows from (4.1) and (4.3) that there exists a fixed point of the Poincaré map on the interval (y_{B_1}, τ), i.e., there exists an order-1 periodic solution for system (1.2).

Similarly, for $A_1(1)$(II), if $y_{T^+} < y_{B_1}$, any solution of system (1.2) will undergo a finite number of impulses, and will not eventually reach the line L_1, which indicates that there is no fixed point for system (1.2). This completes the proof.

□

Theorem 4.2. *For case $A_1(1)$(III), if $y_{T^+} \geq y_{B_1}$, there exists at least one fixed point of the Poincaré map $P_M(y_i^+)$, i.e., there exists at least one order-1 periodic solution for the system (1.2); if $y_{T^+} < y_{B_1}$, then $P_M(y_i^+)$ does not have any fixed point.*

Proof. If $y_{T^+} = y_{B_1}$, the curve $\widehat{B_1T}$ constitutes an order-1 periodic solution of system (1.2). Otherwise, we consider the following two cases:

$$(i)y_{T^+} \geq \tau, \qquad (ii)y_{T^+} < \tau.$$

For case (i), if $y_{T^+} > y_{B_1}$, then $P_M(y_{B_1}) > y_{B_1}$. Moreover, if $y_{T^+} \geq \tau$, any impulsive point is below the point T^+, then we have $P_M(y_{T^+}) < y_{T^+}$. It shows that there exists a fixed point of the Poincaré map $P_M(y_i^+)$ on the interval (y_{B_1}, y_{T^+}).

For case (ii), if $y_{T^+} > y_{B_1}$, then $P_M(y_{B_1}) > y_{B_1}$. If $y_{T^+} < \tau$, $B_\tau = ((1-H)E_T, \tau)$ is the highest impulsive point for which the inequality $P_M(\tau) < \tau$ holds. It shows that there exists a fixed point for the Poincaré map $P_M(y_i^+)$ on the interval (y_{B_1}, τ).

In summary, if $y_T^+ \geq y_{B_1}$, there exists an order-1 periodic solution for system (1.2).

For $y_{T^+} < y_{B_1}$, any solution of system (1.2) will undergo a finite number of impulses and it does not eventually reach the line L_1, which indicates that there is no fixed point for system (1.2). This completes the proof.

□

Theorem 4.3. *For case $A_1(2)$(I) (or case $A_1(2)$(II)), there exists at least one fixed point of the Poincaré map $P_M(y_i^+)$, i.e., there exists at least one order-1 periodic solution for the system (1.2).*

Proof. For case $A_1(2)$(I), there exists a curve τ_2 tangents to the line L_2 at the point C_0 and intersects with the line L_1 at point C_1. If $P_M(y_{C_0}) = y_{C_1}^+ = y_{C_0}$, then the curve $\widehat{C_0C_1}$ constitutes the order-1 periodic solution for system (1.2).

If $y_{C_1}^+ > y_{C_0}$ or $y_{C_1}^+ < y_{C_0}$, the trajectory starting from the point C_1^+ eventually reaches at the line L_1 with a point $C_2 = (E_T, y_{C_2})$ and it is clear that $y_{C_2} < y_{C_1}$. At the same time, the point C_2 undergoes impulsive action and then arrives at the phase set, where the phase point is $C_2^+ = ((1-H)E_T, y_{C_2^+})$. For case $A_1(2)$(I), the impulsive function is monotonically increasing on the interval $[0, y_{C_1}]$, and the Poincaré map $P_M(y_{C_1^+})$ satisfies

$$P_M(y_{C_1^+}) < y_{C_1^+}. \tag{4.4}$$

In addition, the point $B_\tau = ((1-H)E_T, \tau)$ is the lowest impulsive point that satisfies

$$P_M(\tau) > \tau. \tag{4.5}$$

It follows from (4.4) and (4.5) that there exists a fixed point of the Poincaré map $P_M(y_i^+)$ on the interval $(\tau, y_{C_1^+})$, i.e., there exists an order-1 periodic solution for the system (1.2).

For case $A_1(2)$(II), the impulsive function is monotonically decreasing on the interval $[0, y_{C_1}]$. If $y_{C_1}^+ > y_{C_0}$ or $y_{C_1}^+ < y_{C_0}$, the Poincaré map $P_M(y_{C_1^+})$ satisfies

$$P_M(y_{C_1^+}) > y_{C_1^+}. \tag{4.6}$$

In addition, now $B_\tau = ((1-H)E_T, \tau)$ is the highest impulsive point, which satisfied inequality (4.3).

It follows from (4.3) and (4.6) that there exists a fixed point of the Poincaré map $P_M(y_i^+)$ on the interval $(y_{C_1^+}, \tau)$, i.e., there exists an order-1 periodic solution for system (1.2). This completes the proof. □

Theorem 4.4. *For case $A_1(2)$(III), there exists at least one fixed point of the Poincaré map $P_M(y_i^+)$, i.e., there exists at least one order-1 periodic solution for the system (1.2).*

Proof. If $y_{C_1^+} = y_{C_0}$, the curve $\widehat{C_0C_1}$ constitutes the order-1 periodic solution for system (1.2). Otherwise, we consider the following two cases:

$$(i) y_{C_1^+} \geq \tau, \qquad (ii) y_{C_1^+} < \tau.$$

For case (i), if $y_{C_1^+} > y_{C_0}$, then

$$P_M(y_{C_0}) > y_{C_0}. \tag{4.7}$$

By the monotonicity of the impulsive function, the point C_1^+ is the highest impulsive point that satisfies

$$P_M(y_{C_1^+}) < y_{C_1^+}. \tag{4.8}$$

It follows from (4.7) and (4.8) that there exists a fixed point for the Poincaré map $P_M(y_i^+)$ on the interval $(y_{C_0}, y_{C_1^+})$, i.e., there exists an order-1 periodic solution for the system (1.2).

For case (i), if $y_{C_1^+} < y_{C_0}$, on one hand,

$$P_M(y_{C_0}) < y_{C_0}. \tag{4.9}$$

On the other hand, the point $V^+ = ((1-H)E_T, \frac{2\sqrt{\tau\theta}-1}{\theta})$ is the lowest impulsive point, and we have

$$P_M(y_{V^+}) \geq y_{V^+}. \tag{4.10}$$

It follows from (4.9) and (4.10) that there exists a fixed point for the Poincaré map $P_M(y_i^+)$ on the interval (y_{V^+}, y_{C_0}), i.e., there exists an order-1 periodic solution for system (1.2).

For case (ii), if $y_{C_1^+} > y_{C_0}$, then

$$P_M(y_{C_0}) > y_{C_0}. \tag{4.11}$$

Moreover, in this case, the point $B_\tau = ((1-H)E_T, \tau)$ is the highest impulsive point that satisfies inequality (4.3).

It follows from (4.3) and (4.11) that there exists a fixed point for the Poincaré map $P_M(y_i^+)$ on the interval (y_{C_0}, τ), i.e., there exists an order-1 periodic solution for system (1.2).

For case (ii), if $y_{C_1^+} < y_{C_0}$, then

$$P_M(y_{C_0}) < y_{C_0}. \tag{4.12}$$

Furthermore, the point V^+ is the lowest impulsive point that satisfies

$$P_M(y_{V^+}) \geq y_{V^+}. \tag{4.13}$$

It follows from (4.12) and (4.13) that there exists a fixed point for the Poincaré map $P_M(y_i^+)$ on the interval $[y_{V^+}, y_{C_0}]$, i.e., there exists an order-1 periodic solution for system (1.2). This completes the proof. □

Theorem 4.5. *For case A_2(I) (or case A_2(II) and case A_2(III)), there exists at least one fixed point of the Poincaré map $P_M(y_i^+)$, i.e., there exists at least one order-1 periodic solution for the system (1.2).*

The proof is similar to Theorem 4.3 and Theorem 4.4.

After discussing the existence of order-1 periodic solutions under different cases, we will address the stability of the order-1 periodic solutions.

Theorem 4.6. *The order-1 periodic solution $(\xi(t), \eta(t))$ is orbitally asymptotically stable if, and only if,*

$$\left|\frac{(1-\frac{\tau\theta}{(1+\theta\eta_0+\frac{\tau\theta}{1+\theta\eta_0})^2})[(\frac{r_0(1-H)E_T}{1+k(\eta_0+\frac{\tau}{1+\theta\eta_0})})-d(1-H)E_T-a[(1-H)E_T]^2-\frac{p(1-H)E_T(\eta_0+\frac{\tau}{1+\theta\eta_0})}{1+q(1-H)E_T}]}{\frac{r_0E_T}{1+k\eta_0}-dE_T-aE_T^2-\frac{pE_T\eta_0}{1+qE_T}}exp(\int_0^T G(t)dt)\right|<1, \tag{4.14}$$

where

$$G(t)=\frac{r_0}{1+k\xi(t)}-d-2a\xi(t)-\frac{p\eta(t)(1+q\xi(t))-pq\xi(t)\eta(t)}{(1+q\xi(t))^2}+\frac{cp\xi(t)}{1+q\xi(t)}-m.$$

Proof. We discuss the asymptotic stability of order-1 periodic solutions with respect to system (1.2) under the conditions for Theorem 4.3.

By using the Poincaré criterion, first, assuming the order-1 periodic solutions $(\xi(t), \eta(t))$ passes point $C = (E_T, \eta_0)$ and the corresponding impulsive point is $C^+ = ((1-H)E_T, \eta_0 + \frac{\tau}{1+\theta\eta_0})$. The Floquet multiplier μ_2 can be expressed as:

$$\begin{aligned}\mu_2 &= \Delta_1 exp(\int_0^T [\frac{\partial P}{\partial x}(\xi(t),\eta(t))+\frac{\partial Q}{\partial y}(\xi(t),\eta(t))]dt)\\ &= \frac{P_+(\frac{\partial\varphi}{\partial y}\frac{\partial\phi}{\partial x}-\frac{\partial\varphi}{\partial x}\frac{\partial\phi}{\partial y}+\frac{\partial\phi}{\partial x})+Q_+(\frac{\partial\alpha}{\partial x}\frac{\partial\phi}{\partial y}-\frac{\partial\alpha}{\partial y}\frac{\partial\phi}{\partial x}+\frac{\partial\phi}{\partial y})}{P\frac{\partial\phi}{\partial x}+Q\frac{\partial\phi}{\partial y}}exp(\int_0^T G(t)dt)\\ &= \frac{(1-\frac{\tau\theta}{(1+\theta\eta_0+\frac{\tau\theta}{1+\theta\eta_0})^2})[(\frac{r_0(1-H)E_T}{1+k(\eta_0+\frac{\tau}{1+\theta\eta_0})})-d(1-H)E_T-a[(1-H)E_T]^2-\frac{p(1-H)E_T(\eta_0+\frac{\tau}{1+\theta\eta_0})}{1+q(1-H)E_T}]}{\frac{r_0E_T}{1+k\eta_0}-dE_T-aE_T^2-\frac{pE_T\eta_0}{1+qE_T}}exp(\int_0^T G(t)dt)\end{aligned}$$

where

$$G(t)=\frac{r_0}{1+k\xi(t)}-d-2a\xi(t)-\frac{p\eta(t)(1+q\xi(t))-pq\xi(t)\eta(t)}{(1+q\xi(t))^2}+\frac{cp\xi(t)}{1+q\xi(t)}-m.$$

Denote

$$F(y)=(\frac{r_0(1-H)E_T}{1+ky})-d(1-H)E_T-a[(1-H)E_T]^2-\frac{p(1-H)E_Ty}{1+q(1-H)E_T},$$

and it is easy to see that $F'(y)=-(\frac{kr_0(1-H)E_T}{(1+ky)^2}+\frac{p(1-H)E_T}{1+q(1-H)E_T})<0$, so the monotonically decreasing interval of the function $F(y)$ is $(-\infty,+\infty)$.

If $x=(1-H)E_T$, $y=y_{C_0}$, we know that

$$F(y_{C_0})=(\frac{r_0(1-H)E_T}{1+ky_{C_0}})-d(1-H)E_T-a[(1-H)E_T]^2-\frac{p(1-H)E_Ty_{C_0}}{1+q(1-H)E_T}=0.$$

If $y_{C_1^+}=y_{C_0}$, i.e., $F(y_{C_1^+})=F(y_{C_0})=0$, it means that $|\mu_2|=0<1$, and the order-1 periodic solution is orbitally asymptotically stable.

For case $A_1(2)$(I), if $y_{C_1^+}>y_{C_0}$ and point C^+ is below point C_0, by the monotonicity of the impulsive function, then $1-\frac{\tau\theta}{(1+\theta\eta_0+\frac{\tau\theta}{1+\theta\eta_0})^2}>0$, $exp(\int_0^T G(t)dt)>0$, and $F(y_{C^+})>0$, and we can know that $\mu_2>0$.

If $y_{C_1^+} > y_{C_0}$ and point C^+ is above point C_0, then $1 - \frac{\tau\theta}{(1+\theta\eta_0+\frac{\tau\theta}{1+\theta\eta_0})^2} > 0$, $exp(\int_0^T G(t)dt) > 0$, and $F(y_{C^+}) < 0$, and we can know that $\mu_2 < 0$.

For case $A_1(2)$(I), if $y_{C_1^+} < y_{C_0}$, by the monotonicity of the impulsive function, the point C^+ must be below the point C_0 clearly, then $1 - \frac{\tau\theta}{(1+\theta\eta_0+\frac{\tau\theta}{1+\theta\eta_0})^2} > 0$, $exp(\int_0^T G(t)dt) > 0$, and $F(y_{C^+}) > 0$, and we can know that $\mu_2 > 0$.

For case $A_1(2)$(II), if $y_{C_1^+} > y_{C_0}$, by the monotonicity of the impulsive function, the point C^+ must be above the point C_0 clearly, then $1 - \frac{\tau\theta}{(1+\theta\eta_0+\frac{\tau\theta}{1+\theta\eta_0})^2} < 0$, $exp(\int_0^T G(t)dt) > 0$, and $F(y_{C^+}) < 0$, and we can know that $\mu_2 > 0$.

For case $A_1(2)$(II), by the monotonicity of the impulsive function, if $y_{C_1^+} < y_{C_0}$ and point C^+ is above point C_0, then $1 - \frac{\tau\theta}{(1+\theta\eta_0+\frac{\tau\theta}{1+\theta\eta_0})^2} < 0$, $exp(\int_0^T G(t)dt) > 0$, and $F(y_{C^+}) < 0$. We can know $\mu_2 > 0$. If $y_{C_1^+} < y_{C_0}$ and point C^+ is below point C_0, then $1 - \frac{\tau\theta}{(1+\theta\eta_0+\frac{\tau\theta}{1+\theta\eta_0})^2} < 0$, $exp(\int_0^T G(t)dt) > 0$, and $F(y_{C^+}) > 0$, and we can know that $\mu_2 < 0$.

Therefore, if $|\mu_2| < 1$, i.e., the inequality (4.14) holds true, then the order-1 periodic solution $(\xi(t), \eta(t))$ of system (1.2) is orbitally asymptotically stable. Similarly, we can prove that under the conditions of Theorem 4.4 and Theorem 4.5, the order-1 periodic solutions of system (1.2) are also orbitally asymptotically stable. This completes the proof.

□

5. Existence of order-k periodic solutions

In this section, we will discuss the existence of order-k ($k \geq 2$) periodic solutions in some cases for the system (1.2).

Theorem 5.1. *For case $A_1(1)$(II), if the condition $y_{T^+} > y_{B_1}$ is satisfied (or for case $A_1(2)$(I), if the condition $y_{C_1^+} < y_{C_0}$ is satisfied; if the condition $y_{C_1^+} > y_{C_0}$ is satisfied for case $A_1(2)$(III)), then there is no order-k ($k \geq 2$) periodic solution of system (1.2).*

Proof. For case $A_1(1)$(II), if $y_{T^+} > y_{B_1}$, by Theorem 4.1, there exists an order-1 periodic solution on the interval (y_{B_1}, τ) for system (1.2). Without loss of generality, assume that the order-1 periodic solution passes through points $B^+ = ((1-H)E_T, \eta_0^+)$ and $B = (E_T, \eta_0)$. The trajectory starting from the initial point T^+ reaches at the line L_1 with the point $T_1 = (E_T, y_{T_1})$. Since any two trajectories are disjoint, the point T_1 lies below T. Subsequently, after the impulsive action, T_1 will map to the line L_2 at point T_1^+.

If $\frac{\sqrt{\tau\theta}-1}{\theta} \geq y_T$, we know that the impulsive function $f(z_i) = z_i + \frac{\tau}{1+\theta z_i}$ is monotonically decreasing on the interval $[0, y_T]$, so the point T_1^+ lies above the point T^+. By analogy, it can be shown that the point T_{i+1}^+ lies above the point $T_i^+ (i = 1, 2, \cdots, n)$, which indicating that T_i^+ is monotonically increasing, i.e.,

$$y_{B_1} < y_{T^+} < y_{T_1^+} < y_{T_2^+} < \cdots < y_{T_i^+} < \cdots < y_{T_n^+} < \cdots < \eta_0^+ < \tau.$$

In summary, there is no order-k ($k \geq 2$) periodic solution for system (1.2). For case $A_1(2)$(I), if $y_{C_1^+} < y_{C_0}$(or for case $A_1(2)$(III), if $y_{C_1^+} > y_{C_0}$), a similar method can be used to prove that there is no order-k ($k \geq 2$) periodic solution for system (1.2). This completes the proof. □

Theorem 5.2. *For case $A_1(2)$(I), if $y_{C_1^+} > y_{C_0}$ and $y_{C_2^+} \geq y_{C_0}$ (or for case $A_1(2)$(II), if $y_{C_1^+} < y_{C_0}$ and $y_{C_2^+} \leq y_{C_0}$; for case $A_1(1)$(I), if $y_{T^+} > y_{B_1}$ and $y_{T_1^+} \geq y_{B_1}$), then there is no order-k ($k \geq 3$) periodic solution for the system (1.2).*

Proof. For case $A_1(2)$(I), if $y_{C_1^+} > y_{C_0}$ and $y_{C_2^+} = y_{C_0}$, the two curves $\widehat{C_0C_1}$ and $\widehat{C_1^+C_2}$ form an order-2 periodic solution.

If $y_{C_2^+} > y_{C_0}$, the impulsive points of the solutions which start from the interval $[y_{C_2^+}, y_{C_1^+}] \in \mathcal{X}_5$ are higher than the point C_2^+. In fact, any two trajectories are disjoint, it follows that for case $A_1(2)$(I), and we derive

$$y_{C_0} < y_{C_2^+} < y_{C_4^+} < y_{C_3^+} < y_{C_1^+} = P_M(y_{C_0}),$$

where $y_{C_k^+}$ is the ordinate of the point lies on the phase set which corresponds to the trajectory undergoing one pulse from the initial point $C_{k-1}^+ = ((1-H)E_T, y_{C_{k-1}^+})$. Thus, the following relations for the sequence of impulsive points $y_{C_i}^+$ can be obtained:

$$y_{C_0} < y_{C_2^+} < y_{C_4^+} < \cdots < y_{C_{2n}^+} < y_{C_{2n+2}^+} < \cdots < y_{C_{2n+1}^+} < y_{C_{2n-1}^+} < \cdots < y_{C_3^+} < y_{C_1^+} = P_M(y_{C_0}). \tag{5.1}$$

It follows from (5.1) that either there exists a unique $y^* \in [y_{C_2}^+, y_{C_1}^+]$ such that

$$\lim_{n\to\infty} y_{C_{2n}^+} = \lim_{n\to\infty} y_{C_{2n-1}^+} = y^*, \tag{5.2}$$

or there exist two different values $y_1^* \neq y_2^* (y_1^*, y_2^* \in [y_{C_2}^+, y_{C_1}^+])$ such that

$$\lim_{n\to\infty} y_{C_{2n}^+} = y_1^*, \quad \lim_{n\to\infty} y_{C_{2n-1}^+} = y_2^*. \tag{5.3}$$

Therefore, it follows from (5.2) and (5.3) that there exists either a fixed point or a two-point periodic cycle for the Poincaré map $P_M(y_i^+)$. That is, for case $A_1(2)$(I), if $y_{C_1^+} > y_{C_0}$ and $y_{C_2^+} \geq y_{C_0}$, there exist an order-1 periodic solution and order-2 periodic solution for system (1.2), and there is no order-k ($k \geq 3$) periodic solutions.

In a similar way, it can be shown that for case $A_1(2)$(II), if $y_{C_1^+} < y_{C_0}$ and $y_{C_2^+} \leq y_{C_0}$ (or for case $A_1(1)$(I), if $y_{T^+} > y_{B_1}$ and $y_{T_1^+} \geq y_{B_1}$), there is no order-k ($k \geq 3$) periodic solution for system (1.2). This completes the proof. □

6. Numerical simulation

In this section, we will verify the results obtained in the theoretical part and the influence of the fear factor on the dynamics of system (1.2) through numerical simulations. Figures 2 and 3 demonstrate the existence of order-1 and order-2 periodic solutions for system (1.2), respectively. Furthermore, Figures 4, 5, and 6 illustrate higher-order periodic solutions for system (1.2), including an order-3 periodic solution in Figure 4, an order-4 periodic solution in Figure 5, and an order-5 periodic solution in Figure 6. Figures 2 to 6 illustrate the rich dynamic behaviors of system (1.2). Under certain conditions of the integrated control strategy, the populations of pests and predators will display periodic oscillations, maintaining both population densities in a stable state while ensuring that the pest density remains below the economic threshold. In Figures 2 to 6, despite consistent values for the fear factor k, there is variation in the order of periodic solutions. This indicates that the fear factor k is not the only condition

that determines the order of periodic solutions, and it is closely related to other parameters of the system (1.2).

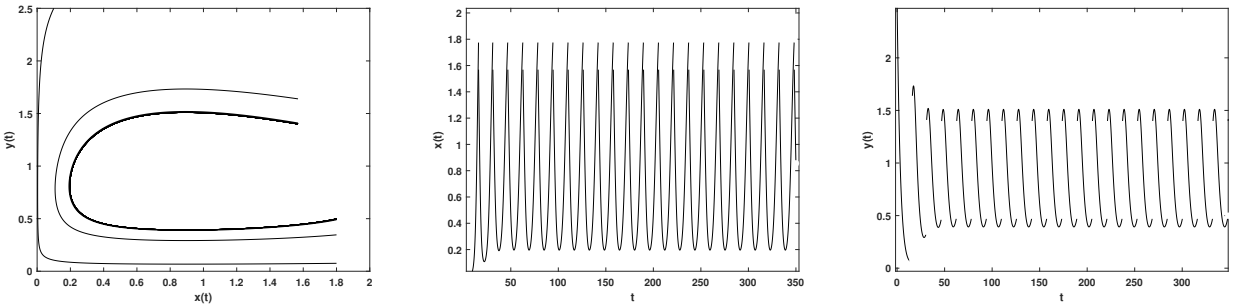

Figure 2. The order-1 periodic solution of system (1.2), where $r_0 = 1$, $a = 0.08$, $k = 0.3$, $p = 1.2$, $c = 0.53$, $d = 0.4$, $m = 0.3$, $q = 1$, $\beta = 1$, $\tau = 1.8$, $\theta = 2$, $\delta = 0.2$, $E_T = 1.8$. (a) Graph of the relationship between x and y; (b) Times series of x; (c) Times series of y.

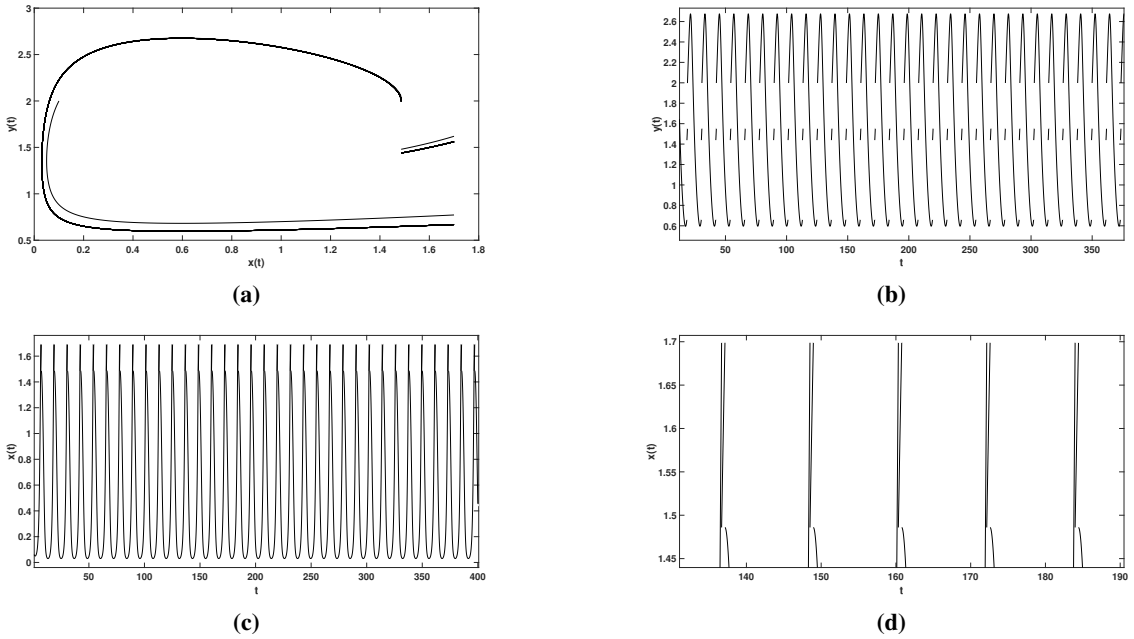

Figure 3. The order-2 periodic solution of system (1.2), where $r_0 = 2$, $a = 0.1$, $k = 0.3$, $p = 1.5$, $c = 0.5$, $d = 0.03$, $m = 0.28$, $q = 1$, $\beta = 1$, $\tau = 1.8$, $\theta = 2$, $\delta = 0.2$, $E_T = 1.7$. (a) Graph of the relationship between x and y; (b) Times series of y; (c) Times series of x; (d) The partial enlargement of (c).

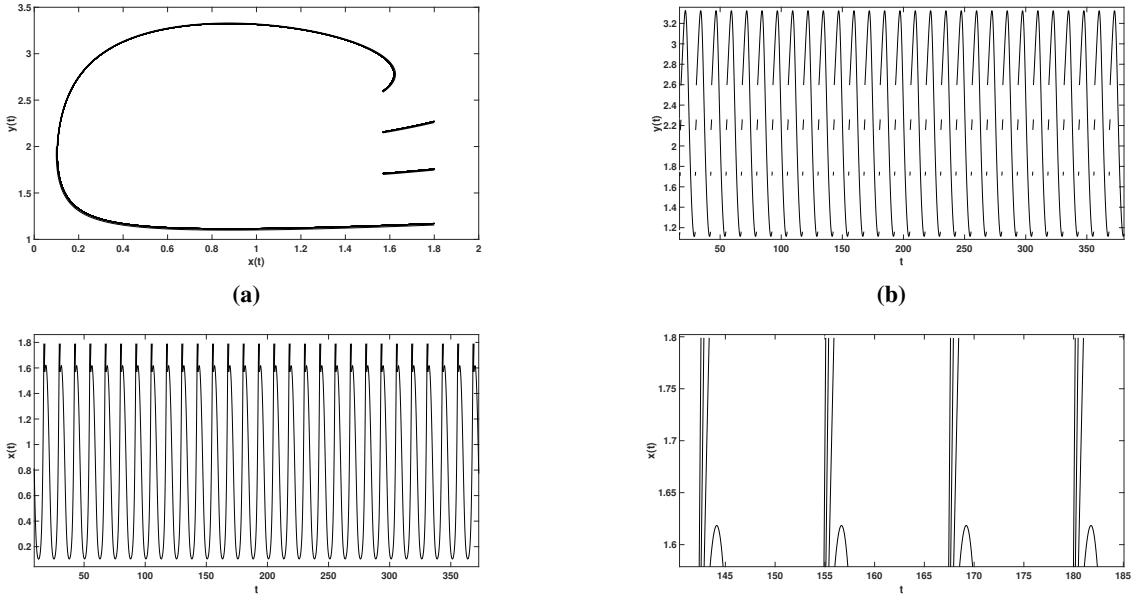

Figure 4. The order-3 periodic solution of system (1.2), where $r_0 = 2.2$, $a = 0.11$, $k = 0.3$, $p = 1.2$, $c = 0.5$, $d = 0.03$, $m = 0.28$, $q = 1$, $\beta = 1$, $\tau = 1.8$, $\theta = 2$, $\delta = 0.2$, $E_T = 1.8$. (a) Graph of the relationship between x and y; (b) Times series of y; (c) Times series of x; (d) The partial enlargement of (c).

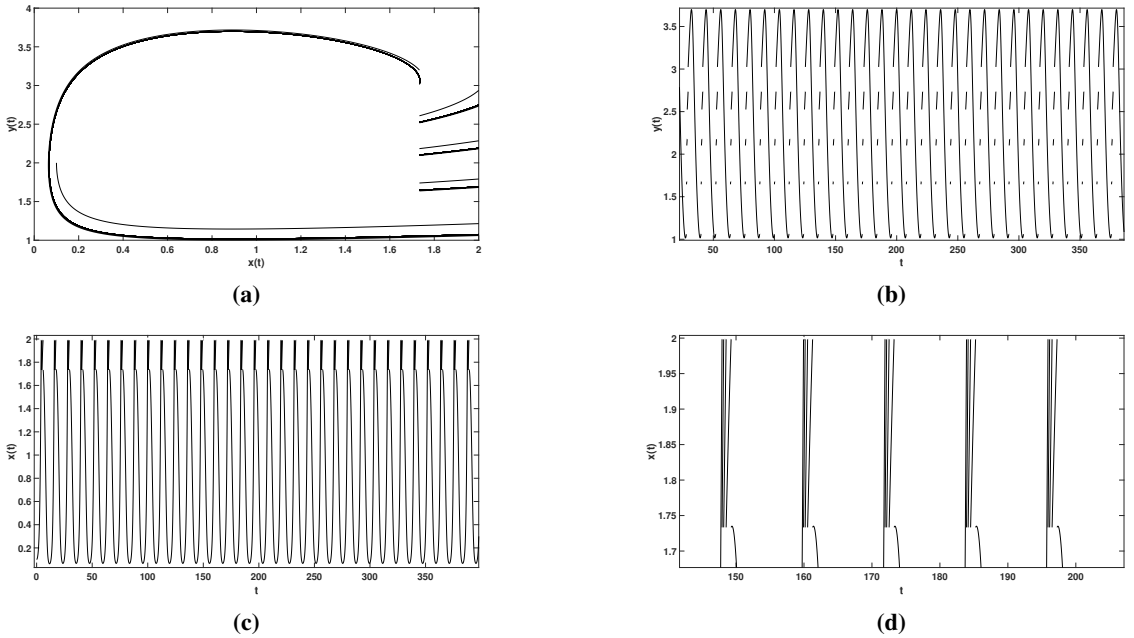

Figure 5. The order-4 periodic solution of system (1.2), where $r_0 = 2.3$, $a = 0.08$, $k = 0.3$, $p = 1.2$, $c = 0.53$, $d = 0.03$, $m = 0.3$, $q = 1$, $\beta = 1$, $\tau = 1.8$, $\theta = 2$, $\delta = 0.2$, $E_T = 2$. (a) Graph of the relationship between x and y; (b) Times series of y; (c) Times series of x; (d) The partial enlargement of (c).

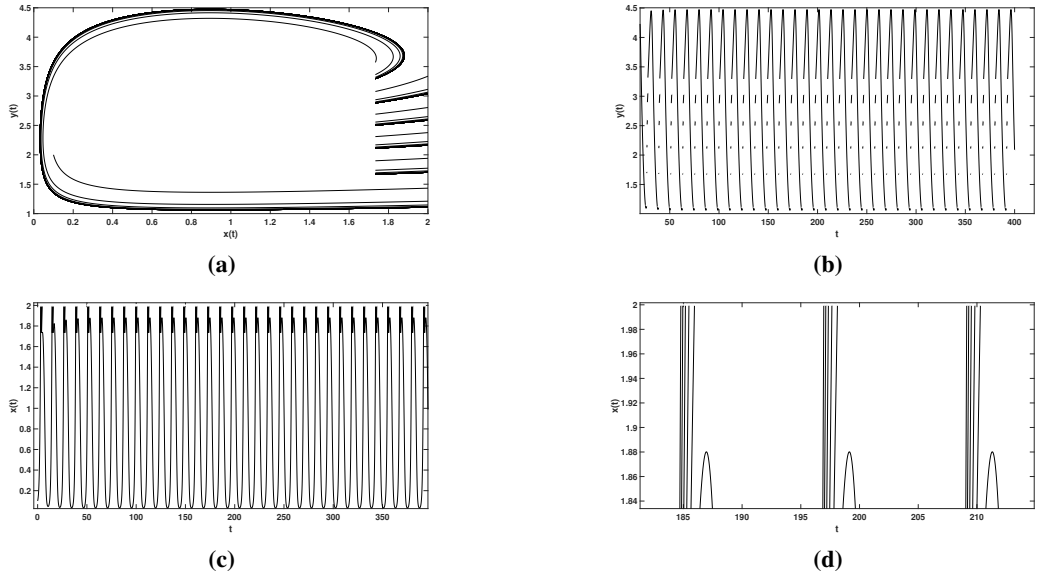

Figure 6. The order-5 periodic solution of system (1.2), where $r_0 = 2.7$, $a = 0.08$, $k = 0.3$, $p = 1.2$, $c = 0.53$, $d = 0.04$, $m = 0.3$, $q = 1$, $\beta = 1$, $\tau = 1.8$, $\theta = 2$, $\delta = 0.2$, $E_T = 2$. (a) Graph of the relationship between x and y; (b) Times series of y; (c) Times series of x; (d) The partial enlargement of (c).

The impact of fear factor on population size is addressed in Figure 7, which reveals important discoveries. Specifically, the graph demonstrates that a decrease in the fear factor leads to an increase in the frequency of oscillations within prey and predator cycles, and their populations remain at relatively high levels. Conversely, an increase in the fear factor intensifies the predator's disruptive influence on prey dynamics, resulting in amplified amplitude of prey cycle oscillations and prolonged decline periods for their populations. These findings align with previous studies and further confirm that predators exert coercive effects on prey by inducing stress responses that impede development and reproduction rates, ultimately leading to population declines. This further implies that the fear effect cannot be ignored in terms of its impact on the population density of pests and predators.

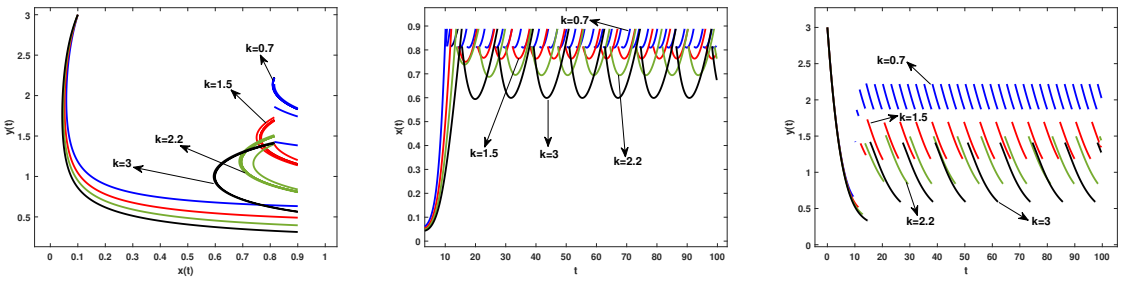

Figure 7. The influence of the fear factor on population size, where $r_0 = 1$, $a = 0.01$, $d = 0.04$, $p = 0.5$, $q = 1$, $c = 0.6$, $m = 0.2$, $E_T = 0.9$, $\delta = 0.2$, $\beta = 1$, $\tau = 1.8$, $\theta = 2$. Here the fear factors are $k = 0.7$, $k = 1.5$, $k = 2.2$ and $k = 3$.

7. Conclusions

The IPM approach combines biological and chemical technologies to offer an economical and efficient ecological solution for controlling plant diseases and insect pests. Moreover, it serves as a foundation for establishing state-dependent impulsive prey-predator models [37–39]. Recently, ecologists and biologists have discovered that the interactions between prey and predators should not be solely described by direct predation, and the fear effect may also play a significant role in predator-prey interactions. When prey becomes aware of the presence of predators, their growth, development, and reproduction are significantly affected. Considering these factors, we propose a nonlinear state-dependent feedback control predator-prey model (1.2) with fear effect, and the aim of this paper is to reveal the dynamical behavior and biological implications of the model.

We used the qualitative theory for impulsive semi-dynamical system to study the impulsive sets and phase sets of system (1.2) under different external conditions if the equilibrium point E_2 is stable, and defined the Poincaré map for impulsive point series in the phase set. The existence and the stability of periodic solutions were discussed by using the principle of successor functions and the Poincaré criteria. Subsequently, numerical simulations were conducted utilizing MATLAB software. The results indicate that the population dynamics of the predator-prey system are influenced by multiple factors, including the initial density of pests and predators, intraspecifics competition, the numbers of released predators, the mortality rate of insecticides, and the fear caused by predators. The global asymptotic stability of periodic solution means that under appropriate control strategies, pests and natural enemies can coexist, the populations reach dynamic equilibrium, and the pest density remains below the economic threshold. In addition, based on previous researches, our study introduces the fear effect as an important biological evolutionary force into the predator-prey model, making the model more practical. Figure 7 shows the impact of different levels of species' fear responses on population size, depicting the changes in the amplitude and frequency of predator-prey population oscillations corresponding to changes in fear levels, demonstrating the undeniable influence of fear effects on biological population interactions.

The model developed in this paper incorporates the natural enemy density regulation factor θ and the fear factor k of prey to predator. The introduction of θ is motivated by the rapid development and application of pest monitoring and early warning technology, as well as information agriculture technology which enhances resource efficiency. The inclusion of the fear factor k objectively reflects a new understanding of human influence on species evolution, leaving ample room for studying the fear effect in species interactions. In fact, some real prey-predator interactions are often neglected when constructing models, such as the anti-predation behavior of adult prey against young predators, the hiding of predators, the aggregation of prey, or the reduction of prey activity, etc. It has been shown in many previous papers that the existence of refuges may have a significant impact on the coexistence of prey and predators [40–42]. Therefore, in the future, we will consider incorporating these factors into mathematical models and conducting the dynamics analysis of them, which will be helpful for designing IPM strategies and making management decisions.

Author contributions

Zhanhao Zhang: Conceptualization, Investigation, Methodology, Validation, Writing-original draft, Data curation, Software; Yuan Tian: Conceptualization, Methodology, Writing-review and editing, Supervision.

Use of AI tools declaration

The authors declare they have not used Artificial Intelligence (AI) tools in the creation of this article.

Acknowledgments

This work was supported by the National Natural Science Foundation of China (NSFCs: 12201196, 12361100) and by the Postgraduate Education Innovation Project in School of Mathematics and Statistics of Hubei Minzu University (STK2023016).

Conflict of interest

All authors declare that they have no competing interests.

References

1. Wangersky, J. Peter, Lotka-Volterra population models, *Annu. Rev. Ecol. Syst.,* **9** (1978), 189–218. https://www.jstor.org/stable/2096748
2. B. Liu, Y. Zhang, L. Chen, Dynamic complexities of a Holling I predator–prey model concerning periodic biological and chemical control, *Chaos Soliton. Fract.,* **22** (2004), 123–134. https://doi.org/10.1016/j.chaos.2003.12.060
3. X. Liu, L. Chen, Complex dynamics of Holling type II Lotka–Volterra predator–prey system with impulsive perturbations on the predator, *Chaos Soliton. Fract.,* **16** (2003), 311–320. https://doi.org/10.1016/S0960-0779(02)00408-3
4. X. Xu, Y. Qiu, X. Chen, H. Zhang, Z. Liang, B. Tian, Bifurcation analysis of a food chain chemostat model with Michaelis-Menten functional response and double delays, *AIMS Math.,* **7** (2022), 12154–12176. https://doi.org/10.3934/math.2022676
5. J. H. P. Dawes, M. O. Souza, A derivation of Holling's type I, II and III functional responses in predator–prey systems, *J. Theor. Biol.,* **327** (2013), 11–22. https://doi.org/10.1016/j.jtbi.2013.02.017
6. T. Namba, Y. Takeuchi, M. Banerjee, Stabilizing effect of intra-specific competition on prey-predator dynamics with intraguild predation, *Math. Model. Nat. Pheno.,* **13** (2018), 29. https://doi.org/10.1051/mmnp/2018033
7. A. Yousef, A. A. Thirthar, A. L. Alaoui, P. Panja, T. Abdeljawad, The hunting cooperation of a predator under two prey's competition and fear-effect in the prey-predator fractional-order model, *AIMS Math.,* **7** (2022), 5463–5479. https://doi.org/10.3934/math.2022303

8. B. Tang, Y. Xiao, Bifurcation analysis of a predator–prey model with anti-predator behaviour, *Chaos Soliton. Fract.,* **70** (2015), 58–68. https://doi.org/10.1016/j.chaos.2014.11.008

9. L. Y. Zanette, A. F. White, M. C. Allen, et al., Perceived predation risk reduces the number of offspring songbirds produce per year, *Science,* **334** (2011), 1398–1401. http://doi.org/10.1126/science.1210908

10. S. Eggers, M. Griesser, J. Ekman, Predator-induced plasticity in nest visitation rates in the Siberian jay (Perisoreus infaustus), *Behav. Ecol.,* **16** (2005), 309–315. https://doi.org/10.1093/beheco/arh163

11. C. K. Ghalambor, S. I. Peluc, T. E. Martin, Plasticity of parental care under the risk of predation: How much should parents reduce care?, *Biol. Letters.,* **9** (2013), 20130154. https://doi.org/10.1098/rsbl.2013.0154

12. F. Hua, J. R. J. Fletcher, K. E. Sieving, R. M. Dorazio, Too risky to settle: avian community structure changes in response to perceived predation risk on adults and offspring, *P. Roy. Soc. B-biol. Sci.,* **280** (2013), 20130762. https://doi.org/10.1098/rspb.2013.0762

13. F. Hua, K. E. Sieving, J. R. J. Fletcher, C. A. Wright, Increased perception of predation risk to adults and offspring alters avian reproductive strategy and performance, *Behav. Ecol.,* **25** (2014), 509–519. https://doi.org/10.1093/beheco/aru017

14. J. J. Fontaine, T. E. Martin, Parent birds assess nest predation risk and adjust their reproductive strategies, *Ecol. Lett.,* **9** (2006), 428–434. https://doi.org/10.1111/j.1461-0248.2006.00892.x

15. S. Creel, D. Christianson, S. Liley, J. A. Winnie, Predation risk affects reproductive physiology and demography of elk, *Science,* **315** (2007), 960–960. http://doi.org/10.1126/science.1135918

16. M. J. Sheriff, C. J. Krebs, R. Boonstra, The sensitive hare: sublethal effects of predator stress on reproduction in snowshoe hares, *J. Anim. Ecol.,* **78** (2009), 1249–1258. https://doi.org/10.1111/j.1365-2656.2009.01552.x

17. A. J. Wirsing, W. J. Ripple, A comparison of shark and wolf research reveals similar behavioral responses by prey, *Front. Ecol. Environ.,* **9** (2011), 335–341. https://doi.org/10.1890/090226

18. M. A. McPeek, M. Grace, J. M. L. Richardson, Physiological and behavioral responses to predators shape the growth/predation risk trade-off in damselflies, *Ecology,* **82** (2001), 1535–1545. https://doi.org/10.1890/0012-9658(2001)082[1535:PABRTP]2.0.CO;2

19. G. Kunert, W. W. Weisser, The interplay between density-and trait-mediated effects in predator-prey interactions: A case study in aphid wing polymorphism, *Oecologia,* **135** (2003), 304–312. https://doi.org/10.1007/s00442-003-1185-8

20. E. B. Mondor, B. D. Roitberg, Pea aphid, Acyrthosiphon pisum, cornicle ontogeny as an adaptation to differential predation risk, *Can. J. Zool.,* **80** (2002), 2131–2136. https://doi.org/10.1139/z02-209

21. Y. Xue, Impact of both-density-dependent fear effect in a Leslie–Gower predator–prey model with Beddington–DeAngelis functional response, *Chaos Soliton. Fract.,* **185** (2024), 115055. https://doi.org/10.1016/j.chaos.2024.115055

22. S. Pal, N. Pal, S. Samanta, J. Chattopadhyay, Effect of hunting cooperation and fear in a predator-prey model, *Ecol. Complex.,* **39** (2019), 100770. https://doi.org/10.1016/j.ecocom.2019.100770

23. Y. Xue, F. Chen, X. Xie, S. Chen, An analysis of a predator-prey model in which fear reduces prey birth and death rates, *AIMS Math.,* **9** (2024), 12906–12927. https://doi.org/10.3934/math.2024630
24. X. Wang, L. Zanette, X. Zou, Modelling the fear effect in predator–prey interactions, *J. Math. Biol.,* **73** (2016), 1179–1204. https://doi.org/10.1007/s00285-016-0989-1
25. J. Mei, S. Wang, X. Xia, W. Wang, An economic model predictive control for knowledge transmission processes in multilayer complex networks, *IEEE. T. Cybernetics.,* **54** (2022), 1442–1455. https://doi.org/10.1109/TCYB.2022.3204568
26. C. Li, S. Tang, Analyzing a generalized pest-natural enemy model with nonlinear impulsive control, *Open. Math.,* **16** (2018), 1390–1411. https://doi.org/10.1515/math-2018-0114
27. J. Mei, S. Wang, D. Xia, J. Hu, Global stability and optimal control analysis of a knowledge transmission model in multilayer networks, *Chaos Soliton. Fract.,* **164** (2022), 112708. http://dx.doi.org/10.1016/j.chaos.2022.112708
28. Y. Tian, S. Tang, R. A. Cheke, Dynamic complexity of a predator-prey model for IPM with nonlinear impulsive control incorporating a regulatory factor for predator releases, *Math. Model. Anal.,* **24** (2019), 134–154. https://doi.org/10.3846/mma.2019.010
29. S. Wang, J. Mei, D. Xia, Z. Yang, J. Hu, Finite-time optimal feedback control mechanism for knowledge transmission in complex networks via model predictive control, *Chaos Soliton. Fract.,* **164** (2022), 112724. http://dx.doi.org/10.1016/j.chaos.2022.112724
30. S. Tang, L. Chen, Modelling and analysis of integrated pest management strategy, *Discrete. Cont. Dyn-B.,* **4** (2004), 759–768. https://doi.org/10.3934/dcdsb.2004.4.759
31. L. S. Chen, H. D. Cheng, Modeling of integrated pest control drives the rise of semi-continuous dynamical system theory, *Int. Math. Model. Appl.,* **10** (2021), 1–16. http://dx.doi.org/10.19943/j.2095-3070.jmmia.2021.01.01
32. P. F. J. Wolf, J. A. Verreet, An integrated pest management system in Germany for the control of fungal leaf diseases in sugar beet: The IPM sugar beet model, *Plant. Dis.,* **86** (2002), 336–344. https://doi.org/10.1094/PDIS.2002.86.4.336
33. S. Tang, R. A. Cheke, State-dependent impulsive models of integrated pest management (IPM) strategies and their dynamic consequences, *J. Math. Biol.,* **50** (2005), 257–292. https://doi.org/10.1007/s00285-004-0290-6
34. X. Song, Z. Xiang, The prey-dependent consumption two-prey one-predator models with stage structure for the predator and impulsive effects, *J. Theor. Biol.,* **242** (2006), 683–698. https://doi.org/10.1016/j.jtbi.2006.05.002
35. J. Yang, S. Tang, Holling type II predator–prey model with nonlinear pulse as state-dependent feedback control, *J. Comput. Appl. Math.,* **291** (2016), 225–241. https://doi.org/10.1016/j.cam.2015.01.017
36. Y. Tian, S. Tang, R. A. Cheke, Nonlinear state-dependent feedback control of a pest-natural enemy system, *Nonlinear. Dynam.,* **94** (2018), 2243–2263. https://doi.org/10.1007/s11071-018-4487-4
37. S. Y. Tang, W. H. Pang, On the continuity of the function describing the times of meeting impulsive set and its application, *Math. Biosci. Eng.,* **14** (2017), 1399–1406. http://dx.doi.org/10.3934/mbe.2017072

38. C. Li, S. Tang, R. A. Cheke, Complex dynamics and coexistence of period-doubling and period-halving bifurcations in an integrated pest management model with nonlinear impulsive control, *Adv. Differ. Equ-NY.,* **2020** (2020), 1–23. https://doi.org/10.1186/s13662-020-02971-9

39. I. U. Khan, S. Y. Tang, The impulsive model with pest density and its change rate dependent feedback control, *Discrete Dyn. Nat. Soc.,* **1** (2020), 4561241. https://doi.org/10.1155/2020/4561241

40. V. Křivan, Effects of optimal antipredator behavior of prey on predator–prey dynamics: The role of refuges, *Theor. Popul. Biol.,* **53** (1998), 131–142. https://doi.org/10.1006/tpbi.1998.1351

41. H. Zhang, Y. Cai, S. Fu, W. Wang, Impact of the fear effect in a prey-predator model incorporating a prey refuge, *Appl. Math. Comput.,* **356** (2019), 328–337. https://doi.org/10.1016/j.amc.2019.03.034

42. H. Molla, S. Sarwardi, M. Haque, Dynamics of adding variable prey refuge and an Allee effect to a predator–prey model, *Alex. Eng. J.,* **61** (2022), 4175–4188. https://doi.org/10.1016/j.aej.2021.09.039

AIMS Press